

## An approach of mapping quarries in Vietnam using low-cost Unmanned Aerial Vehicles

NGUYEN Quoc Long <sup>11\*</sup>, BUI Xuan Nam<sup>2</sup>, CAO Xuan Cuong<sup>1</sup>, LE Van Canh<sup>1</sup>

<sup>1</sup> Hanoi University of Mining and Geology, Department of Mine Surveying, Hanoi, Vietnam

<sup>2</sup> Hanoi University of Mining and Geology, Department of Surface Mining, Hanoi, Vietnam and Mine Surveying, Krakow, Poland

**Abstract.** In Vietnam, there are a huge number of quarries that are exploited and mainly provide materials to the construction sector of the country. However, most of the quarries are operating without topographic plans due to a lack of surveying activities. This paper introduces an approach of using low-cost UAVs to produce digital surface models which in turn are used to draw topographic maps of quarries in Vietnam. For assessments of accuracy, safety, and working efficiency, four quarries different in terrain conditions, namely Luong Son, Long Son, Nui Nho, and Nui Dai were selected as the study areas. Ground control points were established in each area by using GNSS/RTK for camera calibration and accuracy assessment. The accuracy of DSM was assessed using the root-mean-square error (RMSE) in X, Y, Z, XY, and XYZ components. Capturing images from each site were processed by using Agisoft®PhotoScan Professional 1.5.2. The results showed that all the DSM models of the four areas have high accuracy, RMSE on the checked GCPs ranges from 1.0 to 9.0 cm, from 1.2 to 5.0 cm, from 4.4 to 13.4 cm, from 1.6 to 10.3 cm, and from 4.9 to 16.9 cm for X, Y, Z, XY, XYZ components, respectively. We concluded that the low-cost UAV based mapping technology can guarantee the accuracy of DSMs, the safety of UAV flying, and the efficiency of surveying working simultaneously when using in quarries.

### Introduction

Vietnam's mining industry was started by French in the late 19<sup>th</sup> century before being taken by Vietnamese in 1954 [1]. As one of the most important economic activities, the mining industry of Vietnam has been developing at a great pace. There have been approximately 1100 mines under excavation in which nearly two-third are open-pit ones [1]. There are several large size open-pit mines such as Coc Sau, Cao Son, Deo Nai, Nui Beo (coal mines), Sin Quyen (copper mine), the remain of open-pit mines are in small and medium sizes. These mines include quarries that mainly provide materials to the cement production industry and construction in Vietnam.

It is undeniable that topographic documents play an important role in the mining operation. However, while several large coal open-pit mines have frequently topographic surveys, almost every medium and small – sized ones do not. Therefore, these open-pit mines rely on experience to carry out mining operations without topographical maps and accurate mine drawings. There are several possible reasons including relatively lacking capital and skills due to the conditions of one small business which in turn lead to not

---

<sup>1</sup> Corresponding author: [nguyenquoclong@humg.edu.vn](mailto:nguyenquoclong@humg.edu.vn)

acquired surveying equipment and professional surveyors [2]. Recently, the rapid development of geospatial technologies has brought many benefits to the mining surveying. Among the most widely used surveying techniques such as Electronic Distance Measurement (EDM) surveys or Total Station (TS) and RTK Global Navigation Satellite System (GNSS) which are able to obtain observations with millimeter accuracy but cost and time consuming, there have been new alternative techniques for topographic surveying such as Terrestrial Laser Scanning (TLS) and airborne Light Detection and Ranging (LiDAR) or airborne laser scanning (ALS) [3]. However, for these new ones, the cost and survey time are still a critical issue to open-pit mines. For example, as the observation distance of TLS is normally short, many scanning stations are required for the complex terrain of open-pit mines. For LiDAR, it is noted that large uncertainties could be found in vertical values while measuring such complicated open-cast mine environment [4].

In Vietnam, small and medium sized open-pit mines such as quarries are often located in areas with complicated terrains and a variety of geological conditions. Many of them are high limestone mountains, others are at a level of 100 meters below the sea level. The changes of terrain elevation at these mines are significant. These lead to many challenges for surveying services which are conducted by using traditional methods.

Recent advancements in robots and GNSS technologies have provided various Unmanned Aerial Vehicles (UAVs) and UAV photogrammetry is recognized as a technology that can replace or complement existing surveying equipment [5]. Especially, small and low-cost UAVs with nonmetric digital cameras are becoming a valid and effective alternative surveying technique for topographic reconnaissance and volumetric computation [5-7], Civil Engineering ([8], disaster prevention [9, 10], agriculture [11]. In addition, with the possibility of measuring a large area quickly, the UAV technology could be observation solutions for small and medium open-air mine sites in Vietnam.

In this study, we perform investigations on the accuracy of 3D mapping several complex terrain open-pit mines by using the UAV technology. These quarries are with a variety of size and terrain and located in different regions of Vietnam, namely Nui Nho, Long Son, Luong Son, and Nui Dai. In all cases, a DJI Phantom 4 Professional was used to capture images, at different flight heights, whereas ground control points were measured by using GNSS RTK. The image processing was carried out using Agisoft®PhotoScan Professional 1.3. Finally, accuracy assessment for each case was performed and conclusions are given.

## Study areas

The study areas are four quarries with specific characteristics of terrain in the Northern and Southern Vietnam, namely Luong Son, Long Son, Nui Nho, and Nui Dai. While Luong Son and Long Son are located in the northern mountainous region of Vietnam, Nui Nho and Nui Dai are situated in the southern of Vietnam (Fig. 1a). Long Son is a limestone quarry and provides materials for the production of cement, whereas other three mines mainly provide materials for civil construction such as air stations, roads, dams, etc. The area of Long Son quarry is about 12 hectares with the highest point of 110m. The largest difference between the mine and the surrounding area in altitude is about 100 m (Fig. 1b). Luong Son is a mine of construction material stone, with an exploiting area of about 13 hectares with steep rocky topography and the biggest difference in elevation is 110 m. Both Long Son and Luong Son mines are exploited by cutting down from the top.

Nui Dai and Nui Nho are two quarries located in the southern part of Vietnam (Fig. 1a). Nui Dai is one of the biggest quarries in Vietnam with the exploiting area of about 70

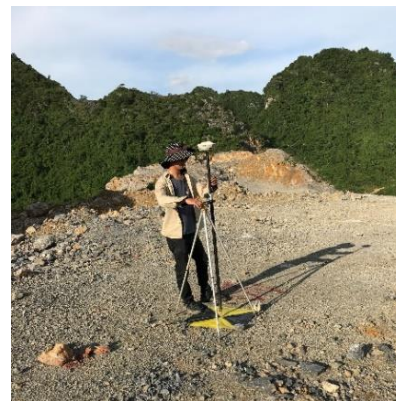
hectares. The highest peak of the mining area is 145 m, the lowest point is at 1 m above sea level. Nui Nho is with an area of 27 ha, and down to the level of -110 m below sea level.

## Materials and Methods

### Principle of UAV based mapping technology

Unmanned aerial vehicles (UAVs) are a generic aircraft design which are intended to operate without a human pilot on board [12]. It has been known with other terms such as remote piloted aircraft or unmanned aerial system. Actually, according to ICAO [13], there are a difference in the two terms. While the latter refers to UAVs that do not allow pilot interventions during the flight and are mainly used in military contexts, the former one refers to unmanned aircraft which are remotely controlled by a pilot [14]. To classify UAVs, one can base on a wide range of different platforms which, due to their physical size, structures and power, differ in terms of their capability and simplicity of operation. These factors impact the payload carrying capacity, speed, altitude, and range of flight, which determines the different applications that can be performed by each type of UAV.

In the field of surveying and mapping, the UAV is classified and summarized based on its structure and type of taking-off and landing operation. There are two main UAVs including fixed-wing and rotary-wing. Fixed-wing unmanned airplanes are flying with air lift and are energy-efficient and can fly for a long time so that a large area can be shot at one time. On the other hand, rotor blades are relatively inefficient. Although the short flight time is short, vertical takeoff and landing are possible, so it can be used in small and medium-sized open-pit mines where it is difficult to secure landings.



(a)



(b)



**Fig. 1.** Location of investigating open-cast mines  
(a) Luong Son; (b) Long Son; (c) Nui Nho; (d) Nui Dai

### UAV and Camera

In small surveying projects, rotary-wing UAVs such as DJI Phantom 3, or 4 professional are often utilized widely. In this work, the study sites are small so we use a phantom 4 professional to capture images. The Phantom 4 professional is a quadcopter drone with four powerful rotors (Fig 2). Its airframe carries the GPS/IMU that enables it to have posture control, stop flight, and automatically take off and land with high stability [15]. The drone is capable of both manual flight mode using the controller and automatic flight mode using the Android or IOS smartphone applications. If you use the automatic mode, you can set the flight path, flight speed, flight altitude, shooting range and overlapping of the photographs, so you can take more aerial photographs. The drone is equipped with a 20 megapixel RGB camera with a focal length of 8.8 mm and sensor a size of 13.2 x 8.8 mm that allows high-resolution aerial photography [16].



**Fig 2.** Description of components of a DJI Phantom 4 Professional [16]

### Establishment of ground control points

Ground control points (GCPs) play an important role in geo-referencing and evaluating the accuracy of the DSM model. Therefore, GCPs need to be placed on the ground before carrying out image acquisition. In the condition that all quarries were still operating, field reconnaissance was conducted to select safe areas for placing these GCPs with a help of a handheld GPS (Mapping v3.8 installed in a Samsung A7 smartphone). The GCPs were

distributed in each study area as much as possible, and they were assigned to positions accessible from the field. The number of GCPs was also different from site to site as it depends on the requirement of accuracy and size of each area (Fig 4).



**Fig. 3** GCP marks and their coordinates measured by GNSS/RTK

In order to easily detect GCPs in acquiring images, the GCPs were marked with highly reflective material for enhancing the contrast. The size of the printed marks was 60 x 60 cm (Fig. 3). In the next step, coordinates (x, y, z) (VN2000/UTM Zone 48 N) for these GCPs were determined using GNSS/RTK and the available horizontal and vertical surveying networks at the mine areas.



(a) Luong Son quarry



(b) Long Son quarry



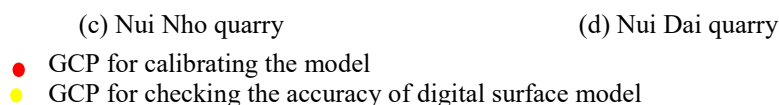


**Fig 4.** Distribution of calibrated and checked points in the four study areas

### UAV image acquisition

For the aerial photography of the study area, the automatic mode flight plan of the Phantom 4 Pro was established using the Pix4D Capture application installed in an IOS smartphone. In the automatic mode, several important parameters are upload to the drone including the size of mapping areas, flight height, as well as end-lap and side-lap of images. As the limitation of flight time, each study area requires several missions to capture enough images for mapping purpose. Table 1 illustrates flying missions of four study areas. In all cases, both forward and side overlaps were set to 80%, but the flight altitudes changed site by site as the change of the study areas' terrain (Table 1). Based on these settings, automatic flight plans were developed to capture aerial photographs in the study areas.

**Table 1.** Flying missions

Name of mine	Flight Altitude (m)	No of mission	No of images	Image resolution (cm/pix)	Area (hectare)
Luong Son	331	6	372	5.36	114
Long Son	303	1	80	5.95	15
Nui Nho	265	7	414	7.48	197
Nui Dai	365	3	215	7.76	121

### Processing and accuracy assessment

In this study, Agisoft Photoscan Professional (ver 1.3) was used to process UAV acquired images taken at the field. The data processing procedure of Agisoft Photoscan includes five steps: (i) photo-alignment; (ii) bundle block adjustment; (iii) optimization, (iv) 3D surface reconstruction, (v) generation of Digital Surface Model (DSM). Firstly, when images are input, key points that can be identified from each image are automatically extracted, and then the singularities extracted from each image are linked with each other through mutual comparison among a plurality of images, this process is called "photo-alignment". When geometric corrections of singularities are completed in each image, the singularities representing the same points in several images are automatically matched through comparison between consecutive UAV images. When the singularities are extracted, 3D point cloud and the DSM model are generated. Also, an orthophoto can be produced through the combination of UAV images.

Accuracy assessment of the Digital Surface Model (DSM) is an important task, and without this task, the DSM is useless. In this project, both the horizontal and vertical assessments were carried out by comparing DSM with the GCPs measured by a Leica total station in term of Root Mean Square Error (RMSE). More specifically, assessments in

easting ( $RMSE_X$ ), northing ( $RMSE_Y$ ), vertical ( $RMSE_Z$ ), and all components ( $RMSE_{XYZ}$ ) were used, as suggested in Agüera-Vega [17], using equations as follows:

$$\Delta X = X_{DSM} - X_{GCP} \quad (1)$$

$$\Delta Y = Y_{DSM} - Y_{GCP} \quad (2)$$

$$\Delta Z = Z_{DSM} - Z_{GCP} \quad (3)$$

$$\Delta XYZ = XYZ_{DSM} - XYZ_{GCP} \quad (4)$$

$$RMSE_X = SQRT \left[ (1/n) \sum_{i=1}^n (\Delta X)^2 \right] \quad (4)$$

$$RMSE_Y = SQRT \left[ (1/n) \sum_{i=1}^n (\Delta Y)^2 \right] \quad (5)$$

$$RMSE_Z = SQRT \left[ (1/n) \sum_{i=1}^n (\Delta Z)^2 \right] \quad (6)$$

$$RMSE_{XYZ} = SQRT \left[ (1/n) \sum_{i=1}^n ((\Delta X)^2 + (\Delta Y)^2 + (\Delta Z)^2) \right] \quad (7)$$

where  $X_{GCP_i}$  and  $X_{DSM}$  are the X-coordinate component of GCP and corresponding coordinate in DSM, respectively;  $Y_{GCP_i}$  and  $Y_{DSM}$  are the Y-coordinate component of GCP and corresponding coordinate in DSM, respectively;  $Z_{GCP_i}$  and  $Z_{DSM}$  are the Z-coordinate component of GCP and corresponding coordinate in DSM, respectively.

## Results and discussions

In term of processing time, an average of 8 hours was spent to process orthographic images and DSMs on a computer with Windows 10 64-bit operating system, 2.93 GHz  $\times$  4 CPU, and 32G RAM.

### Luong Son case

For the case of Luong Son quarry a total of 372 images were acquired through six missions. The point cloud of the quarry with around 20 million 3D points, was extracted according to the data processing method described above, and an orthographic image and a DSM were generated with resolutions of 5.3 and 43.7 cm, respectively. In addition, topographic contours at 1 m intervals could be extracted from the DSM. The results are shown in Fig 5c. The results are shown in Table 2 and 3. The root mean square error (RMSE) of the position coordinates was analyzed to be about 2.0 cm in the horizontal direction and 4.4 cm in the vertical direction

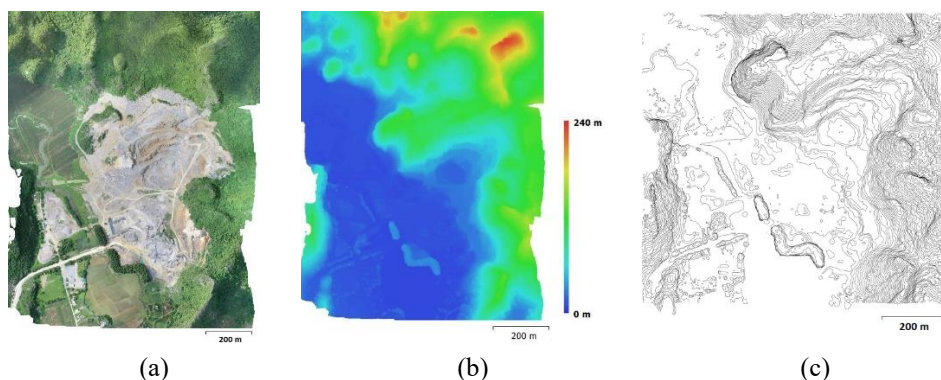


**Fig 5.** Processing results for Luong Son site  
(a) Orthophoto (b) DSM, (c) Contour plan (an interval of 1 m)

**Table 2.** Error and RMSE in X, Y, Z, XY and XYZ of GCPs used for the model calibration

Calibration points	X error (m)	Y error (m)	Z error (m)	XY error (m)	XYZ error (m)
T5	0.007	-0.019	-0.014	0.020	0.024
T6	0.013	0.006	0.001	0.014	0.014
T8	-0.008	-0.020	-0.019	0.022	0.029
T11	0.024	0.010	0.000	0.026	0.026
T12	0.016	0.011	0.091	0.019	0.093
GPS02	0.007	-0.003	0.017	0.008	0.019
GPS03	0.015	0.019	-0.019	0.024	0.031
GPS01	0.013	0.052	0.028	0.053	0.060
T9	-0.019	0.009	0.022	0.021	0.031
<b>RMSE</b>	<b>0.015</b>	<b>0.022</b>	<b>0.035</b>	<b>0.026</b>	<b>0.043</b>

**Table 3.** Error and RMSE in X, Y, Z, XY and XYZ of GCPs used for the checking DSM

Checking points	X error (m)	Y error (m)	Z error (m)	XY error (m)	XYZ error (m)
T1	-0.004	-0.018	-0.072	0.018	0.074
T2	-0.004	-0.006	-0.034	0.007	0.034
T3	-0.032	-0.003	0.026	0.032	0.042
T4	0.006	-0.006	0.022	0.009	0.024
T7	0.000	-0.022	0.012	0.022	0.025
T10	-0.004	-0.009	0.040	0.010	0.041
T13	0.002	0.008	0.012	0.008	0.015
T15	0.019	0.003	0.049	0.019	0.052
T16	-0.025	0.029	-0.078	0.038	0.086
GPS04	-0.002	-0.016	0.041	0.016	0.044
<b>RMSE</b>	<b>0.014</b>	<b>0.015</b>	<b>0.044</b>	<b>0.020</b>	<b>0.049</b>

### Long Son case

For the case of Long Son quarry, with an area of 15 hectares, a total of 80 images were acquired through one mission. The point cloud of the quarry with approximately 3.77 million 3D points, was extracted according to the data processing method described above, and an orthographic image and a DSM were generated with resolutions of 5.9 cm and 23.8 cm/pix, respectively. In addition, topographic contours at 1 m intervals could be extracted from the DSM. The results are shown in Fig 6. The results are shown in Table 4 and 5. The root mean square error (RMSE) of the position coordinates was analyzed to be about 2.6 cm in the horizontal direction and 5.3 cm in the vertical direction.

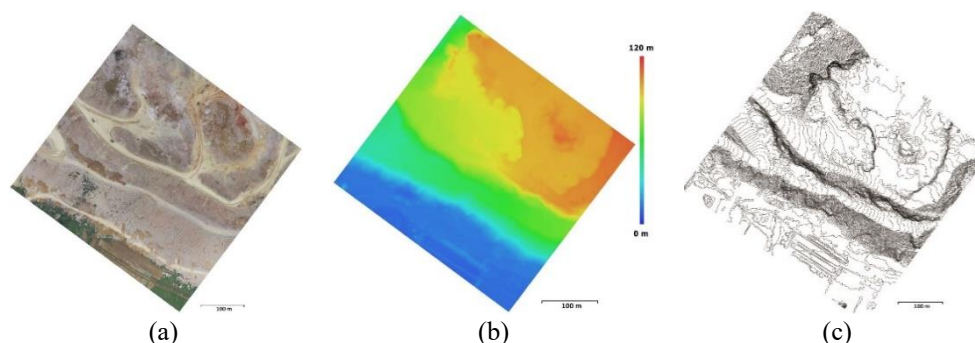


**Fig 6.** Processing results for Long Son site  
(a) Orthophoto (b) DSM, (c) Contour plan (an interval of 1 m)

**Table 4.** Error and RMSE in X, Y, Z, XY and XYZ of GCPs used for the model calibration

Calibration points	X error (m)	Y error (m)	Z error (m)	XY error (m)	XYZ error (m)
A2	-0.006	-0.001	-0.002	0.007	0.007
A3	-0.002	-0.002	0.013	0.002	0.013
A4	0.006	0.005	-0.030	0.008	0.031
A6	0.007	-0.001	0.024	0.007	0.025
A9	-0.007	0.001	-0.008	0.007	0.011
BS1	-0.007	0.005	-0.003	0.009	0.009
BS4	0.005	-0.003	-0.001	0.006	0.006
<b>RMSE</b>	<b>0.007</b>	<b>0.003</b>	<b>0.016</b>	<b>0.007</b>	<b>0.017</b>

**Table 5.** Error and RMSE in X, Y, Z, XY and XYZ of GCPs used for the checking DSM

Checking points	X error (m)	Y error (m)	Z error (m)	XY error (m)	XYZ error (m)
12	0.012	-0.001	0.060	0.012	0.061
23	0.003	0.055	0.011	0.055	0.056
A 5	-0.014	0.003	-0.008	0.014	0.016
A 7	-0.005	0.001	-0.081	0.005	0.081
A 8	-0.010	-0.007	-0.061	0.012	0.062
<b>RMSE</b>	<b>0.010</b>	<b>0.025</b>	<b>0.053</b>	<b>0.026</b>	<b>0.059</b>

### Nui Nho case

For the case of Nui Nho quarry, the largest study area (197 hectares), a total of 414 images were acquired through seven missions. The point cloud of the quarry with 30.818 million 3D points, was extracted according to the data processing method described above, and an orthographic image and a DSM were generated with resolutions of 7.4 and 29.9 cm/pix, respectively. In addition, topographic contours at 1 m intervals could be extracted from the DSM. The results are shown in Fig 7. The results are shown in Table 6 and 7. The root mean square error (RMSE) of the position coordinates was analyzed to be about 10.3 cm in the horizontal direction and 13.4 cm in the vertical direction.

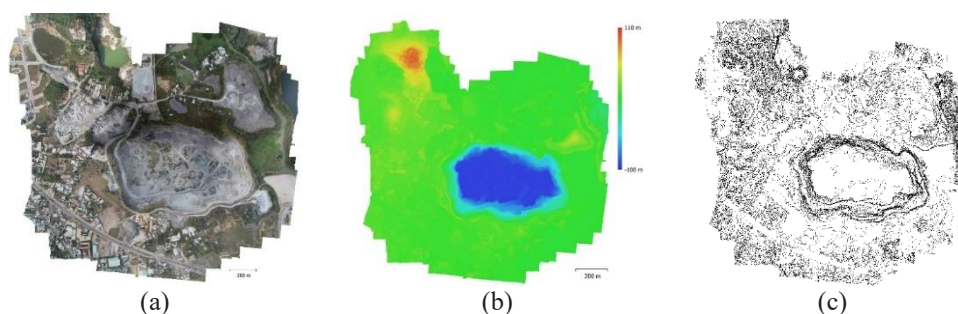


**Fig 7.** Processing results for Nui Nho site  
(a) Orthophoto (b) DSM, (c) Contour plan (an interval of 1 m)

**Table 6.** Error and RMSE in X, Y, Z, XY and XYZ of GCPs used for the model calibration

Calibration points	X error (m)	Y error (m)	Z error (m)	XY error (m)	XYZ error (m)
T4	0.000	-0.001	0.000	0.001	0.002
T1	-0.001	-0.001	0.000	0.001	0.001
T6	-0.003	-0.003	0.001	0.005	0.005
T7	-0.004	0.002	0.000	0.005	0.005
T8	-0.002	0.003	-0.001	0.004	0.004
T10	0.002	0.005	0.000	0.005	0.005
T13	0.007	0.002	0.002	0.007	0.008
T12	-0.002	0.007	-0.004	0.007	0.008
T16	0.003	-0.001	0.001	0.003	0.003
T19	-0.001	-0.005	-0.002	0.005	0.006
T24	0.009	-0.005	0.001	0.010	0.010
T25	0.009	0.002	-0.001	0.009	0.009
T22	-0.017	-0.004	0.001	0.018	0.018
<b>RMSE</b>	<b>0.007</b>	<b>0.004</b>	<b>0.002</b>	<b>0.007</b>	<b>0.008</b>

**Table 7.** Error and RMSE in X, Y, Z, XY and XYZ of GCPs used for the checking DSM

Checking points	X error (m)	Y error (m)	Z error (m)	XY error (m)	XYZ error (m)
T3	-0.086	0.013	-0.005	0.087	0.087
T23	0.004	-0.001	0.038	0.004	0.038

T5	-0.241	-0.010	-0.396	0.241	0.464
T9	-0.019	0.008	0.041	0.020	0.045
T11	-0.007	0.054	0.018	0.055	0.058
T17	0.062	-0.126	0.013	0.141	0.141
T20	-0.044	-0.052	0.017	0.068	0.070
T26	0.000	-0.004	0.035	0.004	0.035
T27	-0.047	0.017	0.004	0.050	0.050
<b>RMSE</b>	<b>0.090</b>	<b>0.050</b>	<b>0.134</b>	<b>0.103</b>	<b>0.169</b>

### Nui Dai case

For the case of Luong Son quarry, with an area of 121 hectares, a total of 215 images were acquired through six missions. The point cloud of the quarry with 16.37 million 3D points, was extracted according to the data processing method described above, and an orthographic image and a DSM were generated with resolutions of 7.7 and 31 cm/pix, respectively. In addition, topographic contours at 1 m intervals could be extracted from the DSM. The results are shown in Fig 8. The results are shown in Table 9 and 10. The root mean square error (RMSE) of the position coordinates was analyzed to be about 1.6 cm in the horizontal direction and 8.4 cm in the vertical direction

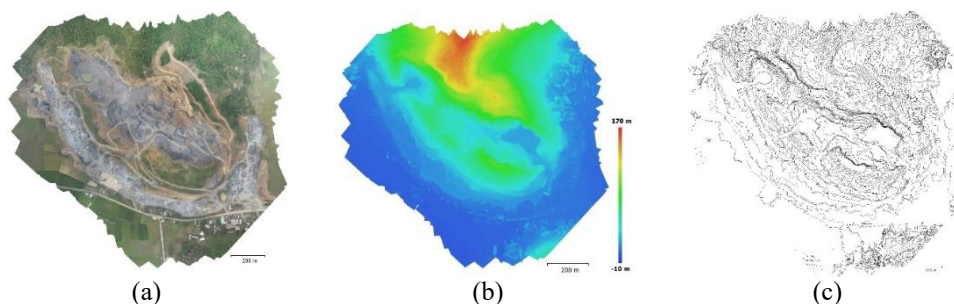


**Fig 8.** Processing results for Nui Dai site  
(a) Orthophoto (b) DSM, (c) Contour plan (an interval of 1 m)

**Table 9.** Error and RMSE in X, Y, Z, XY and XYZ of GCPs used for the model calibration

Calibration points	X error (m)	Y error (m)	Z error (m)	XY error (m)	XYZ error (m)
G5	-0.028	-0.015	0.012	0.031	0.034
G3	-0.019	0.003	0.074	0.019	0.076
G9	-0.011	-0.004	-0.005	0.011	0.012
G8	-0.006	-0.008	-0.047	0.010	0.048
G1	0.024	0.000	-0.024	0.024	0.034
G4	0.015	0.022	-0.016	0.027	0.031
G7	-0.028	0.010	0.004	0.030	0.030
G11	-0.030	0.016	-0.083	0.034	0.089
G12	0.019	-0.007	0.099	0.020	0.101
G18	0.011	-0.023	-0.004	0.026	0.026

G20	0.008	-0.009	0.038	0.012	0.040
G14	0.000	0.007	0.000	0.007	0.007
G15	0.000	0.000	-0.001	0.000	0.001
G16	0.000	0.000	0.000	0.000	0.000
<b>RMSE</b>	<b>0.018</b>	<b>0.012</b>	<b>0.044</b>	<b>0.021</b>	<b>0.049</b>

**Table 10.** Error and RMSE in X, Y, Z, XY and XYZ of GCPs used for the checking DSM

Checking points	X error (m)	Y error (m)	Z error (m)	XY error (m)	XYZ error (m)
GPS 01	0.013	-0.001	-0.026	0.013	0.029
G2	0.008	0.023	0.040	0.024	0.047
G6	-0.004	0.006	-0.034	0.007	0.035
G10	-0.020	0.012	-0.084	0.023	0.087
G13	-0.001	-0.001	-0.179	0.002	0.179
G17	-0.009	-0.019	-0.081	0.021	0.083
G19	-0.006	-0.007	0.018	0.009	0.020
<b>RMSE</b>	<b>0.010</b>	<b>0.012</b>	<b>0.084</b>	<b>0.016</b>	<b>0.086</b>



(a) Luong Son quarry



(b) Long Son quarry



(c) Nui Nho quarry



(d) Nui Dai quarry

**Fig 9.** 3D visualization of the four study areas using the orthophotos and DSMs

## Discussions

One of important input parameters that needs to be set while developing flight plans is the flight height. It is undeniable that this factor should be seriously considered as it influences on several important issues such as DSM's accuracy, the safety of UAV flying

and the efficiency of UAV mapping. In the four study cases, the flight height ranging from 150 m to 250 m ensures the safety of flying, the accuracy of final topographic plans, and the working efficiency. Specifically, the case of Luong Son quarry which is the most complicated terrain among the four study sites. With the flight altitude was set to 331 m, the drone's safety was ensured. While one may question the accuracy, the results show that the MRSEs of XY and X are 2.1 and 4.6 cm, respectively. In other words, this completely meets the accuracy requirement of the detailed survey. In addition, with an average of 15 minutes per mission, the flying time of Luong Son case was only 1.5 hours. Another complex terrain quarry is Nui Dai, with the maximum and minimum elevations are +145m m and +1 m, respectively. However, with the flight elevation of 365 m, a total of 45 minutes spent on flying, the RMSEs of XY and Z (in checking dataset) are 1.6 and 8.4 cm, respectively, indicating the success of field work. For the case of Long Son quarry, as the smallest area of 12 hectares, only one flight mission was carried out to capture images. The accuracy of its DSM is high, and RMSE in checking dataset is 5.3 cm and 2.6 cm for vertical and horizontal, respectively. The lowest accuracy was seen in the DSM of Nui Nho quarry, RMSE in checking dataset is 10.3 cm and 13.4 cm for vertical and horizontal. From the above analysis, the UAV technology shows its efficiency in mapping small sized open-pit mines.

## Conclusions

In this research, an assessment of potential application of low cost UAVs for producing DSM and topographic plans at small and medium sized mine areas with four case studies at Luong Son, Long Son, Nui Nho, and Nui Dai quarries, in Vietnam. Accordingly, a lightweight and small DJI Phantom 4 Professional equipped by the nonmetric RGB Sony EXMOR camera was used. For calibration of the camera and accuracy assessment of DSMs, GCPs were established and determined XYZ coordination (VN2000/UTM Zone 48 N) using a GNSS/RTK CHC X20 with the horizontal accuracy of 5 mm + 1 ppm and the vertical accuracy of 10 mm + 2 ppm.

In order to guarantee the accuracy of DSMs, the safety of UAV flying, and the efficiency of surveying working simultaneously, the flight height for missions was set to from 150 to 250 m with taking terrain conditions into account.

The result showed that the DSM model of Luong Son, the most complicated terrain quarry, has high accuracy though the flight elevation was set to 331 m; the high success-rate of fit was confirmed through RMSEs in the calibrating dataset, 2.6 cm and 3.5 cm for vertical and horizontal, respectively, whereas RMSE in the checking dataset is 4.6 cm and 2.1 cm for vertical and horizontal, indicating high accuracy.

These indicate that the processes of capturing images, establishment of GCPs, and photogrammetric processing were carried out successfully. In addition, in this study, the low-cost rotary-wing drone can be used to survey a small scale and complex terrain quarry quickly. Also, it can be operated by a small number of surveyors, about two people. Therefore, it is considered that this small drone can replace or supplement existing surveying equipment and can be practically used at quarries.

## Acknowledgements

Paper was presented during the 5th POL – VIET International Conference Scientific-Research Cooperation between Vietnam and Poland, 08-10.07.2019, AGH UST, Krakow,

Poland. And this research was supported by the Research Center for Mining Electro-Mechanics of Hanoi University of Mining and Geology.

## 1. References

1. Tran, X.H. and A.T. Nguyen. *Innovation, Modernization, exploitation, screening, production in order to achieve the sustainable development of Coal and Minerals Industry. in Vietnam National Mining Science and Technology Congress*. 2011. Nha Trang, Vietnam.
2. Lee Sungjae and C. Yosoon, *opographic survey at small-scale open-pit mines using a popular rotary-wing unmanned aerial vehicle (drone)*. *Tunnel & Underground Space*, 2015. **25**.
3. Tien Bui, D., et al. *Lightweight Unmanned Aerial Vehicle and Structure-from-Motion Photogrammetry for Generating Digital Surface Model for Open-Pit Coal Mine Area and Its Accuracy Assessment*. 2018. Cham: Springer International Publishing.
4. Jonathan L. Carrivick, Mark W. Smith, and D.J. Quincey, *Structure from Motion in the Geosciences*. 2016: Wiley.
5. Siebert, S. and J. Teizer, *Mobile 3D mapping for surveying earthwork projects using an Unmanned Aerial Vehicle (UAV) system*. *Automation in Construction*, 2014. **41**: p. 1-14.
6. Cryderman, C., S.B. Mah, and A. Shufletoski, *Evaluation of UAV Photogrammetric Accuracy for Mapping and Earthworks Computations*. *GEOMATICA*, 2014. **68**(4): p. 309-317.
7. Clapuyt, F., V. Vanacker, and K. Van Oost, *Reproducibility of UAV-based earth topography reconstructions based on Structure-from-Motion algorithms*. *Geomorphology*, 2016. **260**: p. 4-15.
8. Park, M.H., S.G. Kim, and S.Y. Choi, *The study about building method of geospatial informations at construction sites by unmanned aircraft system (UAS)*. *Journal of the Korean Cadastre Information*, 2013. **15**(1): p. 145-156.
9. Birk, A., et al.
10. Niethammer, U., et al., *UAV-based remote sensing of the Super-Sauze landslide: Evaluation and results*. *Engineering Geology*, 2012. **128**: p. 2-11.
11. Zarco-Tejada, P.J., et al., *Tree height quantification using very high resolution imagery acquired from an unmanned aerial vehicle (UAV) and automatic 3D photo-reconstruction methods*. *European Journal of Agronomy*, 2014. **55**(C): p. 89-99.
12. ICAO, *Unmanned Aircraft Systems (UAS)*, I.C.A. Organization, Editor. 2011: ICAO: Montreal, QC, Canada.
13. ICAO, *Manual on Remotely Piloted Aircraft Systems (RPAS)*, I.C.A. Organization, Editor. 2015: ICAO: Montreal, QC, Canada.
14. Stöcker, E.C., et al., *Review of the current state of UAV regulations*. *Remote sensing*, 2017. **9**(5): p. urn:issn:2072-4292.
15. Ajayi, O.G., et al., *Generation of accurate digital elevation models from UAV acquired low percentage overlapping images*. *International Journal of Remote Sensing*, 2017. **38**(8-10): p. 3113-3134.

16. DJI, *Phantom 4 Pro Visionary intelligence and elevated imagination*, <https://www.dji.com/phantom-4-pro>. 2017.

17. Agüera-Vega, F., F. Carvajal-Ramírez, and P. Martínez-Carricondo, *Accuracy of Digital Surface Models and Orthophotos Derived from Unmanned Aerial Vehicle Photogrammetry*. *Journal of Surveying Engineering*, 2016: p. 04016025.

Dr Paweł CŹWIĄKAŁA AGH

Prof. Hana Stankowa VSB Ostrava